Osimertinib, an Irreversible Next-Generation EGFR Tyrosine Kinase Inhibitor, Exerts Antitumor Activity in Various Preclinical NSCLC Models Harboring the Uncommon EGFR Mutations G719X or L861Q or S768I

Nicolas Floc'h[1,*], Sangbin Lim[2,*], Sue Bickerton[1], Afshan Ahmed[3], Jonathan Orme[3], Jelena Urosevic[1], Matthew J. Martin[1], Darren A.E. Cross[4], Byoung Chul Cho[5], and Paul D. Smith[1]

ABSTRACT

Osimertinib is an oral, third-generation, irreversible epidermal growth factor receptor tyrosine kinase inhibitor (EGFR-TKI) that selectively inhibits both EGFR-TKI–sensitizing and *EGFR* T790M–resistance mutations with lower activity against wild-type EGFR and has demonstrated efficacy in non–small cell lung cancer (NSCLC) CNS metastases. The sensitizing mutations, the in-frame deletions in exon 19 and the L858R point mutation in exon 21, represent between 80% and 90% of all EGFR mutations. The remaining 10% to 20% are referred to as uncommon activating mutations and are a diverse group of mutations in exons 18 to 21 within the kinase domain of the EGFR gene. Excluding those found as insertion mutations in exon 20, the uncommon mutations involving codons G719, S768, and L861 are the most prevalent.

Although the efficacy of EGFR-TKIs for the common EGFR mutations is well established, much less is known about rare EGFR mutations, such as exon 20 insertions, G719X, L861Q, S768I, as most of the data consist of single case reports or small case series.

Using available patient-derived xenografts (PDX) and cell lines derived from two of these PDXs that harbor the G719X mutation, we have evaluated *in vitro* and *in vivo* the preclinical activity of osimertinib. We report osimertinib inhibits signaling pathways and cellular growth in G719X-mutant cell lines *in vitro* and demonstrate sustained tumor growth inhibition of PDX harboring the G719X mutation alone or in combination with L861Q and S768I.

Together, these data support clinical testing of osimertinib in patients with uncommon EGFR NSCLC.

Introduction

The common activating mutations ex19del and L858R account for between 80% and 90% of the activating mutations in EGFR associated with non–small cell lung cancer (NSCLC). The remaining 10% to 20% are referred to as uncommon activating mutations and are a diverse group of mutations in exons 18 to 21 within the kinase domain of the EGFR gene (1, 2). Excluding those found as insertion mutations in exon 20, the uncommon mutations involving codons G719, S768, and L861 are the most prevalent (3–7). The G719X point mutations, where "X" represents any of the possible substitutions, account for collectively 2% to 5% of EGFR-mutated tumors (COSMIC 2018), and result in amino acid substitutions within exon 18 of EGFR at codon position 719 glycine (G): primarily glycine to alanine (G719A), glycine to cysteine (G719C), and glycine to serine (G719S). Mutations affecting G719 can occur alone or in compound mutations with other uncommon mutations, such as S768I or L861Q (3–7). The S768I point mutation accounts for 1.5% to 3% of untreated EGFR-mutated tumors (3–7) and results in amino acid substitution within exon 20 in EGFR at codon position 768, from a serine (S) to an isoleucine (I). The L861Q point mutation accounts for approximately 2% to 3% of EGFR-mutated tumors (3–7) and results in amino acid substitution within exon 21 in EGFR at codon position 861, from a leucine (L) to a glutamine (Q). These uncommon mutations as well as numerous, less prevalent mutations have been detected in NSCLC, and many of these have been reported as both activating and sensitive to EGFR tyrosine kinase inhibitors (TKI) including osimertinib (8).

However, the clinical effectiveness of EGFR-TKI treatment in patients with these uncommon mutations remains unclear because few clinical trials have enrolled patients with G719X, L861Q, or S768I (3, 9–13). To date, the largest clinical study specially designed to evaluate the responses of gefitinib and erlotinib treatment in NSCLC patients with G719X, L861Q, and S768I was composed of 78, 57, and 7 patients, respectively (9). Patients with EGFR Ex19del or L858R point mutations who had been treated with EGFR-TKIs during the same period were selected as the control group. The trial revealed that patients with exon 19 deletions had the most favorable progression-free survival (PFS; median, 13.5 months) and an overall response rate (ORR) of 65.3%, followed by those with L858R (median, 10.4 months; ORR, 67.5%), L861Q (median, 8.1 months; ORR, 39.6%), G719X (median, 6.3 months; ORR, 36.8%), and S768I (ORR, 33.3%) mutations (9). Additionally, compound mutations in 19 patients (G719X; L861Q in 9 patients and G719X;S768I in 10 patients) were evaluated with ORR of 88.9% and 50.0%, respectively.

[1]AstraZeneca Oncology R&D, Research and Early Development, Bioscience, Cambridge, UK. [2]Severance Biomedical Science Institute, Yonsei University College of Medicine, Seoul, Republic of Korea. [3]AstraZeneca Oncology R&D, Research and Early Development, Discovery Science, Cambridge, UK. [4]Global Medical Affairs, Global Medicines Development, AstraZeneca, Cambridge, UK. [5]Division of Medical Oncology, Yonsei Cancer Center, Yonsei University College of Medicine, Seoul, Korea.

Note: Supplementary data for this article are available at Molecular Cancer Therapeutics Online (http://mct.aacrjournals.org/).

*These authors have contributed equally and should be considered as co-first authors.

Corresponding Author: Nicolas Floc'h, AstraZeneca, Robinson Way, Cambridge CB2 0RE, UK. Phone: 01223769654; E-mail: nicolas.floch@astrazeneca.com

Mol Cancer Ther 2020;19:2298–307

doi: 10.1158/1535-7163.MCT-20-0103

Yang and colleagues retrospectively reviewed patients with the G719X, L861Q, or S768I mutations alone or in combination who were treated with the second-generation EGFR-TKI, afatinib, in the LUX-LUNG trial series and found that the ORR was 77.8%, 56%, and 100%. The PFS was 13.8, 8.2, and 14.7 months, respectively (14).

Osimertinib is an oral, third-generation, irreversible EGFR-TKI that selectively inhibits both EGFR-TKI–sensitizing and EGFR T790M–resistance mutations with lower activity against wild-type EGFR and has demonstrated efficacy in NSCLC CNS metastases (15–19). When used in the first-line setting to treat patients with NSCLC harboring the canonical Ex19del or L858R mutations, osimertinib has shown more favorable treatment outcomes than first-generation and second-generation EGFR-TKIs including in patients with CNS metastases (20). Recently, a paper by Ahn and colleagues shows that osimertinib demonstrated favorable activity with manageable toxicity in patients with NSCLC harboring uncommon EGFR mutations (10). Thirty-six patients with uncommon mutations were evaluated, and the objective response rate was 50% with a median PFS of 8.2 months.

Using *in vitro* cellular EGFR phosphorylation assays, we showed that osimertinib was potent against a range of uncommon mutant variants observed clinically of EGFR involving codons G719, S768, L861, and L747. Using available patient-derived xenografts (PDX) and cell lines derived from two of these PDXs that harbor G719X mutation, we have evaluated *in vitro* and *in vivo* the preclinical activity of osimertinib. We report osimertinib inhibits signaling pathways and cellular growth in G719X-mutant cell lines *in vitro* and demonstrates sustained tumor growth inhibition of PDX harboring G719X mutation in combination with L861Q or S768I.

This work demonstrates that osimertinib is active against a range of uncommon mutant variants of EGFR and offers potential to improve treatment options for patients with NSCLC whose tumors harbor an uncommon EGFR mutation.

Materials and Methods

Cell lines

Cos-7 cells were obtained from European Collection of Authenticated Cell Cultures (ECACC). Cos-7 cells were cultured in Dulbecco's Modified Eagle's Medium (DMEM, Sigma-Aldrich) supplemented with 10% fetal calf serum (FCS; PAA) and 1% Glutamax (Life Technologies). Cos-7 cells were authenticated at AstraZeneca cell banking using DNA fingerprinting short tandem repeat assays and confirmed to be free of bacterial and viral contaminations by IDEXX. All cell lines were used within 15 passages and for a period of less than 6 months. The patient-derived cell lines YU-1092 and YU-1099 were derived from malignant effusions of NSCLC patients (21). Both cells were initially cultured on collagen-coated plates in a serum-free defined medium (ACL-4) supplemented with 5% FBS. The cells maintained the driver oncogenes that were observed in the patients. When cells were enriched in an epithelial cell adhesion molecule (EpCAM)-positive cell population with purity of over 95%, cells were subjected to further assays. All patient samples were obtained after written informed consent from the patients using protocols approved by the institutional review board.

Compounds

Osimertinib, AZ5104, and afatinib have been synthetized by AstraZeneca. The synthesis and structures of osimertinib and AZ5104 have been previously reported as compounds 8 and 27 in ref. 22.

In vitro EGFR phosphorylation assays

EGFR phosphorylation was measured using a modified Cisbio Pan phospho-EGFR Cellular Assay Kit. All Cos-7 cells were revived in culture flasks for 16 hours in DMEM supplemented with 10% FCS. Cos-7 cells were detached using TrypLE Express Enzyme (Life Technologies) from culture flasks and resuspended, 5 μL of cell suspension at densities between 600 and 1,400 cells per well was dispensed into a Greiner low volume 384 proxi plates predosed with titrations of test compound, and incubated for 2 hours at room temperature. The cells were stimulated for the final 10 minutes with 200 ng/mL of EGF. Following the 2-hour incubation, 2 μL of the XL665 and Cryptate-labeled antibodies diluted in lysis buffer were added to the cells and incubated for 2 hours at room temperature. Plates were then read on Pherastar with a HTRF module. IC_{50} values were determined following 2-hour incubation with compound titrations. Data were exported to Genedata Screener software package (Genedata) to generate sigmoidal dose−response curves, and an IC_{50} value was generated by determining the compound concentration at which there was a 50% inhibition in signal.

Immunoblot analysis

Bim, EGFR, p-EGFR (Y1068), AKT, pAKT (S473), ERK, pERK (T202/Y204), S6, pS6 (S240/244), and horseradish peroxidase (HRP)–conjugated secondary antibodies were purchased from Cell Signaling Technology. Actin was obtained from Merck Millipore. HRP-dependent luminescence was developed with SuperSignal West Pico Chemiluminescent Substrate (Thermo Fisher Scientific) and detected with LAS-4000 lumino-image analyzer system (Fujifilm).

Proliferation assay

Cells were seeded at a density of 5,000 cells per well on 6-well plates. Cells were incubated overnight and exposed to the indicated drugs for 14 days. Medium containing drugs were replenished every 3 days. Then, cells were stained with crystal violet and counted using ImageJ software.

Xenograft studies

All animal studies were conducted in accordance with UK Home Office legislation, the Animal Scientific Procedures Act 1986, as well as the AstraZeneca Global Bioethics policy. Randomization of animals onto study was based on initial tumor volumes to ensure equal distribution across groups. A power analysis was performed whereby group sizes were calculated to enable statistically robust detection of tumor growth inhibition (≥ 5 per group) or pharmacodynamics endpoint (≥ 4 per group).

For the LC-F-29 (Xentech), the CTG-1082 and CTG-2534 (Champions Oncology) and LU1901 (Crown Bioscience) PDX models, tumor fragments from donor mice inoculated with primary human lung cancer tissues were harvested and inoculated subcutaneously into the flank of nude female mice. Tumor growth was monitored twice weekly by bilateral caliper measurements and tumor volume calculated using the formula TV (cm^3) = [length (cm) × width $(cm)^2$] × 0.5, where the length and the width are the longest and the shortest diameters of the tumor.

Mice were randomized into vehicle or treatment groups with approximate mean start size of 0.2 cm^3. Randomization for animal studies was based on initial tumor volumes to ensure equal distribution across groups. Mice were dosed daily by oral gavage for the duration of the treatment period with vehicle, osimertinib, afatinib, or savolitinib. Tumor growth inhibition (%TGI) from the start of treatment was assessed by comparison of the geometric mean change in tumor

volume for the control and treated groups using the formula: %TGI = $(1 - \{T_t/T_0/C_t/C_0\}/1 - \{C_0/C_t\}) \times 100$, where T_t is the geomean tumor volume of treated at time t, T_0 is the geomean tumor volume of treated at time 0, C_t is the geomean tumor volume of control at time t, and C_0 is the geomean tumor volume of control at time 0. Tumor regression was calculated as the percentage reduction in tumor volume from baseline value: % regression = (1 − RTV) × 100 %, where RTV = mean relative tumor volume. Statistical significance was evaluated using a one-tailed t test.

For pharmacodynamic studies, mice were randomized at a tumor volume between 0.4 and 0.6 cm^3 using the same randomization criteria as the tumor growth inhibition studies. Mice were then treated orally with a single bolus dose of either vehicle, osimertinib, or afatinib. Tumors were excised at specific time points after dosing and flash frozen in liquid nitrogen.

In all *in vivo* studies, osimertinib, afatinib, and savolitinib were administered via oral gavage. Osimertinib, afatinib, and savolitinib were suspended in 0.5% HPMC, 0.5% HPMC + 0.1% polysorbate 80, and carboxymethylcellulose-sodium, pH 2.1, respectively.

Immunoblotting

For *ex vivo*, pea-sized fragments of xenograft tissue were homogenized in the FastPrep-24 5G instrument (MP Bio) in lysis buffer supplemented with protease and phosphatase inhibitor cocktails (Sigma). Homogenates were briefly sonicated using Diagenode Bioruptor plus before 10-minute centrifugation and protein quantification with Pierce protein assay (Thermo Fisher). For all samples, equal protein amounts were loaded for SDS-PAGE using 4% to 12% gradient Bis-Tris precast gels (Novex Life Technologies), followed by transfer to nitrocellulose membranes using the iBlot2 dry transfer system (Novex Life Technologies). After blocking in 5% milk-TBST or BSA-TBST, membranes were blotted with phospho-EGFR (p-EGFR; Tyr1068; Cell Signaling Technology; 2234), total EGFR (tEGFR; Cell Signaling Technology; 2232), phospho-AKT (pAKT; Ser473; Cell Signaling Technology; 4060), total AKT (tAKT; Cell Signaling Technology; 9272), phospho-ERK p(ERK) (Thr202/Tyr204; Cell Signaling Technology; 9101), total ERK (tERK; Cell Signaling Technology; 9102), phospho-S6RP (pS6; Ser235/236, Cell Signaling Technology; 4858), total S6RP t(S6RP) (Cell Signaling Technology; 2217), or vinculin (Sigma; V9131) followed by HRP-conjugated secondary antibodies (Cell Signaling Technology; 7074 or 7076). Signals were detected with SuperSignal West Dura detection reagents (Thermo Fisher). Western blots were developed using G: Box chemi genius instrument (Syngene), and where indicated, signal was quantified in Syngene Genetools software. Protein levels were then normalized to the levels of loading control (vinculin), and treatment groups were normalized to the mean of time-matched vehicle groups. Statistical significance was evaluated using a one-way, two-sided ANOVA.

Results

Osimertinib inhibits EGFR phosphorylation of different uncommon EGFR mutations *in vitro*

To assess the potency of osimertinib against uncommon EGFR mutations, COS7 cells were transfected with cDNAs encoding EGFR G719A/C/S, L861Q, S768I, and L747S as single or compound mutations and treated with increasing concentrations of either osimertinib, AZ5104 (a circulating metabolite of osimertinib), or afatinib to determine the apparent geomean IC_{50} for inhibition of phosphorylation of the uncommon mutants (**Table. 1**). Osimertinib was able to inhibit EGFR phosphorylation of all the uncommon mutations evaluated when expressed individually or in combination with apparent geomean IC_{50} values ranging from 4.5 to 40.7 nmol/L. Osimertinib potency was similar to AZ5104 potency (apparent geomean IC_{50} range, 1.2–40.7) and afatinib potency (apparent geomean IC_{50} range, 1.7–79.2; **Table. 1**). Notably, the potency against uncommon mutations was of the same order as potency in the same assay for inhibition of the common exon 19 deletion and L858R mutants (apparent geomean IC_{50} are of 8.4 and 11.9 nmol/L, respectively; **Table. 1**).

Collectively, these data indicate that osimertinib potently inhibits the activity of multiple different uncommon EGFR mutations *in vitro*.

Osimertinib inhibits EGFR phosphorylation and proliferation of patient-derived tumor cell lines harboring the EGFR G719C/S768I or L861Q mutation *in vitro*

Next, we evaluated the activity of osimertinib to inhibit EGFR phosphorylation and proliferation *in vitro* of EGFR-mutant NSCLC patient-derived cell lines carrying either the EGFR G719C/S768I

Table 1. Summary of inhibition of EGFR phosphorylation by osimertinib, AZ5104, and afatinib in COS7 cells expressing uncommon EGFR mutants.

	Osimertinib Geomean $IC_{50} \pm$ SE (nmol/L)	*n*	AZ5104 Geomean $IC_{50} \pm$ SE (nmol/L)	*n*	Afatinib Geomean $IC_{50} \pm$ SE (nmol/L)	*n*
Cos 7 EGFR G719A	35.4 ± 15.0	2	14.1 ± 0.4	2	9.8 ± 0.4	3
Cos 7 EGFR G719C	19.4 ± 8.1	2	11.6 ± 1.8	3	39.1 ± 130.4	3
Cos 7 EGFR G719S	35.1 ± 14.4	2	40.7 ± 15.5	3	79.2 ± 421.4	3
Cos 7 EGFR L816Q	14.8 ± 4.7	3	6.4 ± 0.6	3	3.6 ± 0.1	3
Cos 7 EGFR S768I	24.0 ± 8.0	3	10.2 ± 0.6	3	4.3 ± 0.3	3
Cos 7 EGFR G719A;L861Q	37.0 ± 8.3	2	20.0 ± 2.3	3	11.7 ± 0.6	2
Cos 7 EGFR G719A;S768I	35.2 ± 7.0	3	11.3 ± 2.2	3	8.3 ± 2.0	2
Cos 7 EGFR G719C;L861Q	11.2 ± 5.0	2	2.3 ± 0.9	3	1.9 ± 0.2	3
Cos 7 EGFR G719C;S768I	4.5 ± 2.1	2	1.7 ± 0.2	2	1.2 ± 0.0	3
Cos 7 EGFR G719S;L861Q	17.5 ± 5.4	2	5.3 ± 0.7	2	6.2 ± 0.5	3
Cos 7 EGFR G719S;S768I	40.7 ± 4.0	3	10.6 ± 0.3	2	9.2 ± 2.2	3
Cos 7 L747S	20.0 ± 5.9	3	7.6 ± 0.5	3	3.8 ± 0.2	3
EGFR Ex19del control line	8.4 ± 1.7	6	7.2 ± 0.7	5	16.7 ± 71	5
L858R control line	11.9 ± 2.1	7	8.7 ± 0.6	6	7.7 ± 0.9	6

Note. Data are represented as apparent IC_{50} geomean ± SE (nmol/L); *n*, number of replicates.

(YU-1099) or the EGFR L861Q (YU-1092) mutations. In the YU-1099, the lowest concentration of osimertinib tested was sufficient to completely inhibit EGFR phosphorylation (**Fig. 1A**). In the YU-1092, osimertinib concentration required to completely inhibit EGFR phosphorylation was between 30 and 100 nmol/L (**Fig. 1B**). Therefore, consistent with engineered COS7 cell data (**Table. 1**), osimertinib inhibits EGFR phosphorylation of representative uncommon EGFR mutations in more disease-relevant cell models. In both cell lines,

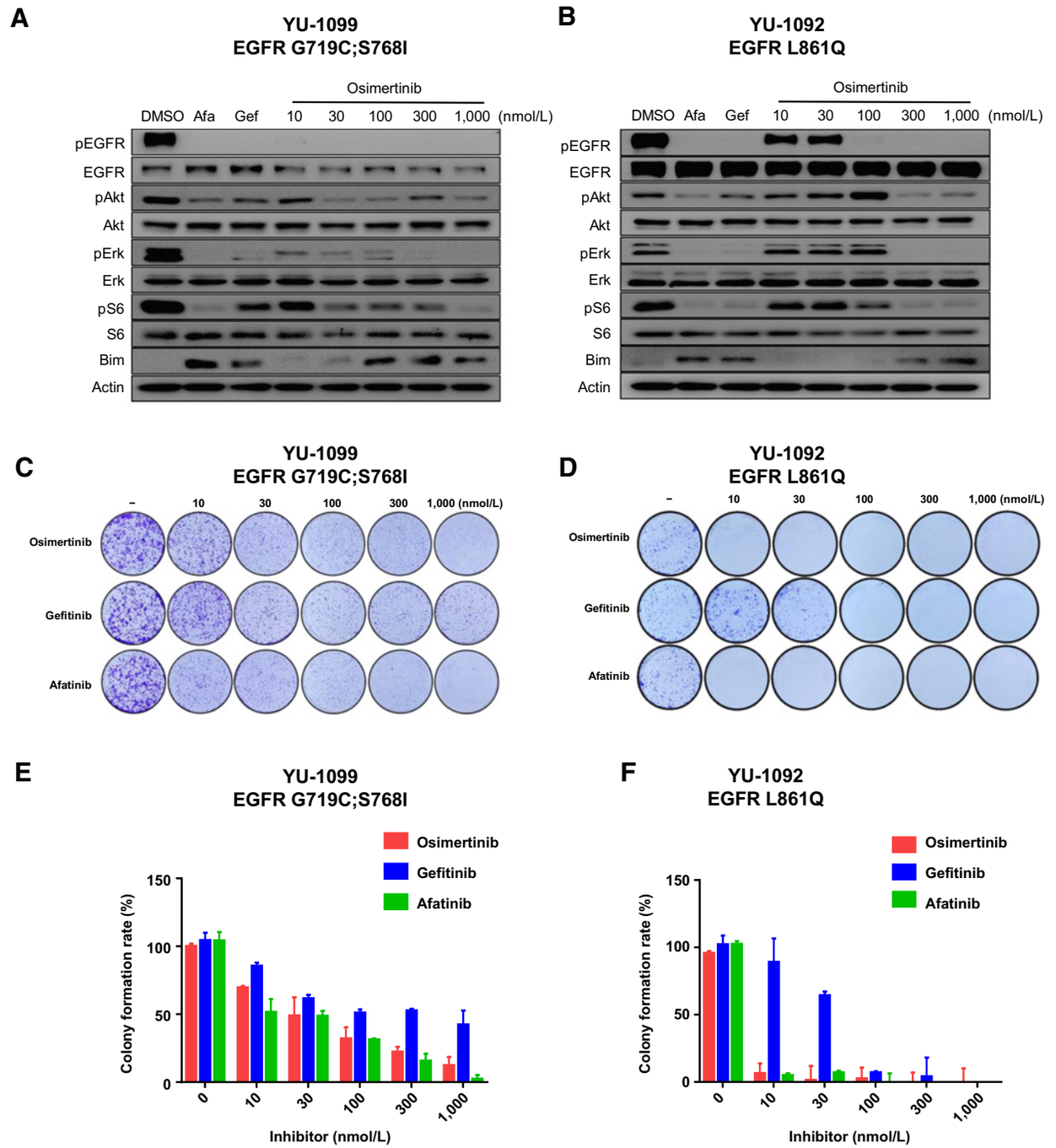

Figure 1.

Osimertinib inhibits the level of p-EGFR and downstream signaling pathways, which translates into proliferation inhibition of the patient-derived cells YU-1099 (EGFR G719C;S768I) and YU-1092 (EGFR L861Q) *in vitro*. Western blots showing P-EGFR and its downstream effector inhibition following 2 hours of osimertinib treatment in a dose-response manner in the (**A**) YU-1099 (EGFR G719C;S768I) and (**B**) YU-1092 (EGFR L861Q) patient-derived cells. DMSO, untreated control; Afa, afatinib 100 nmol/L; Gef, gefitinib 1 μmol/L. **C** and **D,** Representative images and (**E** and **F**) quantification of crystal violet staining in the YU-1099 and YU-1092 cells following EGFR-TKI treatments.

osimertinib induced concentration-dependent inhibition of downstream signaling markers (pAkt, pERK, and pS6) and increase in the levels of the proapoptotic protein BIM (**Fig. 1A** and **B**).

We then explored how the activity against EGFR uncommon mutations translated into cell proliferation inhibition. In line with the phosphorylation data, in a proliferation assay using both the YU-1099 and YU-1092 cell lines, osimertinib showed potent inhibition of proliferation with an apparent IC_{50} of approximately 30 nmol/L and less than 10 nmol/L, respectively (**Fig. 1C–F**).

Osimertinib induces tumor growth inhibition in the LC-F-29 EGFR G719A;S768I PDX model *in vivo*

To explore the *in vivo* activity of osimertinib, we administered the drug as monotherapy against the LC-F-29 NSCLC PDX model that carries the EGFR G719A;S768I mutation. Once-daily administration of 25 mg/kg of osimertinib (a dose that approximates to the clinically approved 80-mg dose) induced significant tumor growth regression in the LC-F-29 PDX model ((>100) 45%, $P < 0.001$ at day 14) when compared with the control group (**Fig. 2A**). A dose of 7.5 mg/kg afatinib, which represents the 40-mg clinical starting dose of afatinib, induces a modest tumor growth inhibition (58%, $P < 0.01$ at day 14) when compared with the control group (**Fig. 2A**). In a repeat of the previous experiment, in the LC-F-29 PDX model, osimertinib induces a very similar tumor regression (>100; 81%, $P < 0.001$ at day 14) when compared with the control group (Supplementary Fig. S1A). Waterfall plots (**Fig. 2B**; Supplementary Fig. S1B) for each of the individual mice treated on these studies demonstrate that all mice experienced reduction in their tumor volumes following osimertinib treatment, whereas all the mice in the afatinib-treated cohort had tumor growth by day 14 (**Fig. 2B**). Both compounds were well tolerated and minimal body weight loss (less than 10% of starting body weight) was observed (**Fig. 2C**; Supplementary Fig. S1C).

Osimertinib inhibits EGFR phosphorylation and downstream signaling pathways in the LC-F-29 EGFR G719A;S768I PDX model *in vivo*

To explore the relationship between efficacy and target modulation, mice bearing LC-F-29 PDX tumors were treated with a single dose of either vehicle, osimertinib, or afatinib, and tumors were harvested 1, 6, 16, and 24 hours later. Comprehensive EGFR pathway biomarkers were used to assess the impact of EGFR-TKI within the tumor tissue (**Fig. 3**). Pharmacodynamics effects were confirmed by assessing phospho-EGFR inhibition by Western blot (**Fig. 3A** and **3E**; Supplementary Fig. S2A), and downstream signaling pathway inhibition by assessing phospho-ERK, phospho-S6, and phospho-AKT inhibition by immunoblotting (**Fig. 3B–E**; Supplementary Fig. S2B–S2D). Although the pharmacokinetic half-life of osimertinib in mice is only approximately 3 hours (15), phospho-EGFR levels remained significantly reduced even 24 hours after dose (**Fig. 3A** and **E**; Supplementary Fig. S2A), consistent with the expected irreversible mode of action. Importantly, downstream signaling markers also showed significant inhibition. All pharmacodynamic biomarkers assessed showed more transient modulation by afatinib than osimertinib, which is consistent with the differences in antitumor efficacy observed in this model (**Fig. 3B–D**; Supplementary Fig. S2B–S2D).

These data demonstrate that osimertinib can achieve robust pathway inhibition *in vivo* of EGFR-mutant NSCLC PDX carrying the EGFR G719A;S768I that is associated with tumor growth inhibition.

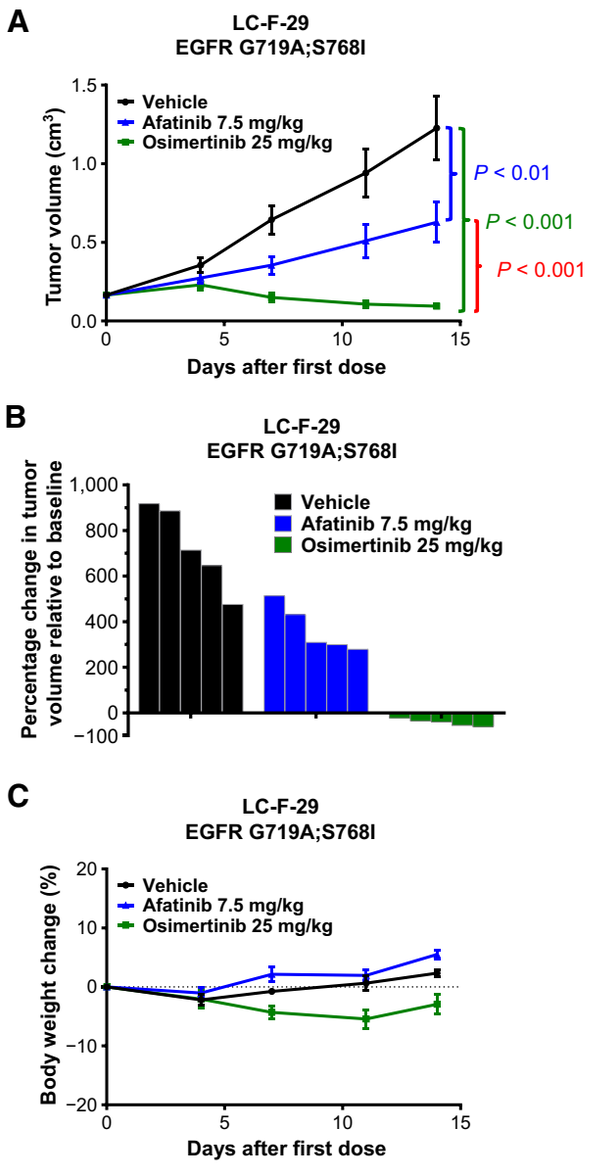

Figure 2.

Osimertinib monotherapy induces tumor growth inhibition in an NSCLC EGFR G719A;S768I mutation PDX model *in vivo*. **A,** Tumor growth inhibition following daily dosing of vehicle, osimertinib 25 mg/kg, or afatinib 7.5 mg/kg in the subcutaneous LC-F-29 PDX model in nude mice. **B,** Waterfall plot representing tumor volume of individual mice at the end of the treatment period. **C,** No significant body weight loss (less than 10% of starting body weight) is observed at these efficacious doses. Data expressed as percentage change in nude mouse body weight relative to start size on day 0. Data are represented as mean ± SEM ($n = 5$ per group).

Osimertinib induces stasis or regression in two PDX models *in vivo* harboring the EGFR G719A;L861Q or G719C;S768I compound mutations

To explore further the *in vivo* activity of osimertinib against G719X mutation in the presence of co-occurring mutations, we administered osimertinib as a monotherapy against the CTG-1082 and CTG-2543 NSCLC PDX models that carry the EGFR G719A;L861Q or the EGFR

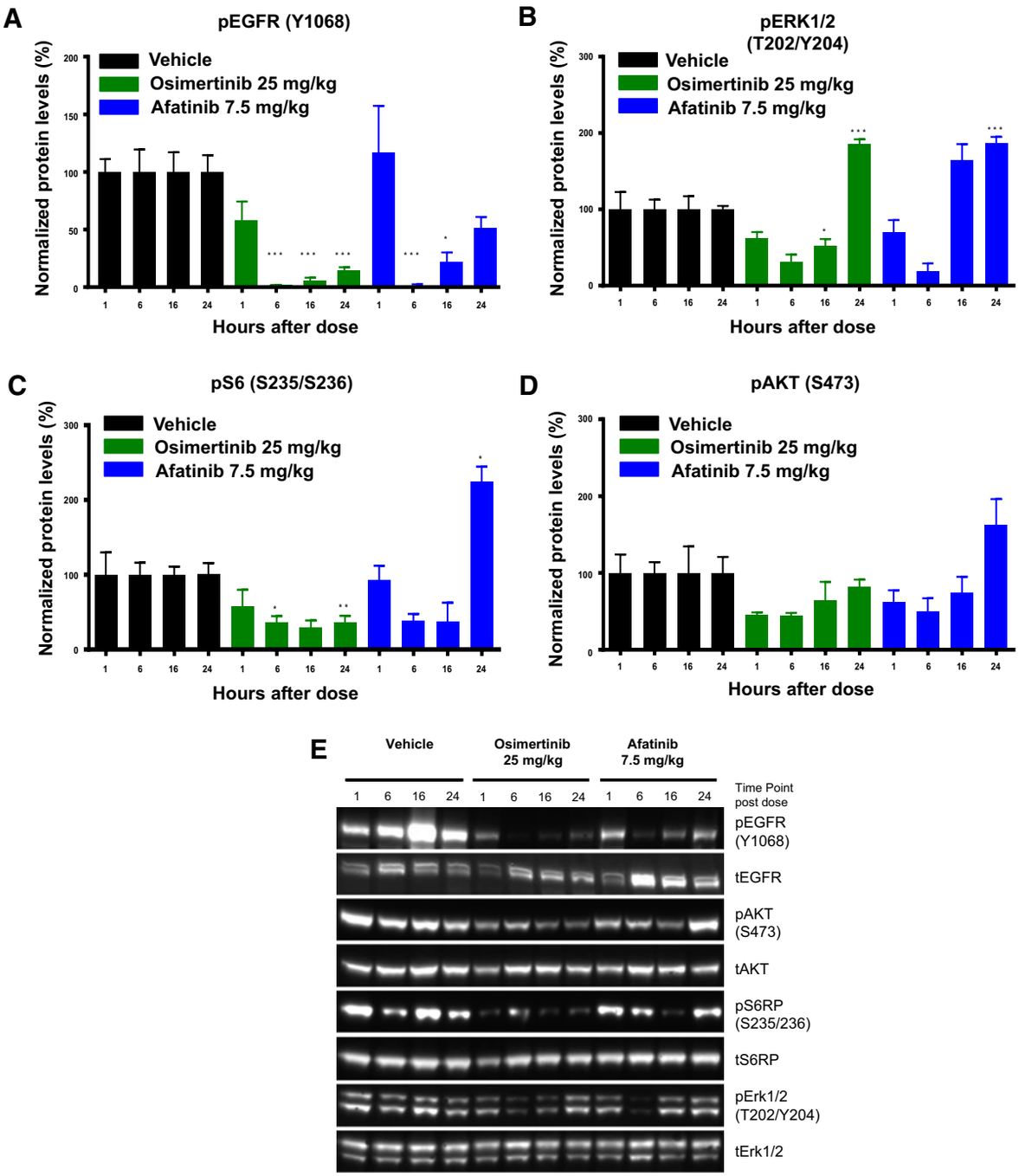

Figure 3.

Osimertinib as monotherapy induces a stronger inhibition of the level of p-EGFR and the downstream signaling pathways than afatinib. Quantification of the level of (**A**) p-EGFR, (**B**) pERK1/2, (**C**) pS6, or (**D**) pAKT determined by immunoblot on tumors collected 1, 6, 16, and 24 hours following one dose of either vehicle, osimertinib, or afatinib. Data are represented as mean ± SEM ($n = 4$ for vehicle and treated groups). **E,** Immunoblot of one representative individual tumor from the various time points with the indicated antibodies. *, $P < 0.05$; **, $P < 0.01$.

G719C;S768I compound mutations, respectively. Once-daily administration of 25 mg/kg of osimertinib induced significant tumor growth inhibition (87%, $P < 0.001$ at day 14) and tumor regression (>100; 58%, $P < 0.001$ at day 14) when compared with the control group in the CTG-1082 and CTG-2543, respectively (**Fig. 4A** and **B**). Waterfall plots for each of the individual mice treated with osimertinib demonstrate that in the CTG-1082 PDX model, half of the mice show stable disease and half of the mice had modest tumor growth (**Fig. 4C**), whereas in the CTG-2534 model, all the mice experienced profound reduction in their tumor volumes by day 14 (**Fig. 4D**).

Osimertinib was well tolerated, and minimal body weight loss (less than 10% of starting body weight) was observed compared with predose starting body weight (**Fig. 4E** and **F**).

Collectively, these results demonstrate that osimertinib is active *in vivo* across PDX models, which harbor the G719X mutation even when co-occurring with either the EGFR L861Q or EGFR S768I and further support the potential efficacy of osimertinib in patients harboring various EGFR uncommon mutant tumors.

Resistance to osimertinib due to MET amplification is overcome by the MET inhibitor savolitinib *in vivo*

LU1901, which harbors the G719A EGFR mutation, was resistant to osimertinib treatment (**Fig. 5A**; Supplementary Fig. S3). Genomic analysis revealed that the model also harbors an amplification of MET, a well-established resistance mechanism known to bypass EGFR inhibition and impart resistance to EGFR-TKIs, including osimertinib (23). To validate the mechanism of resistance, we

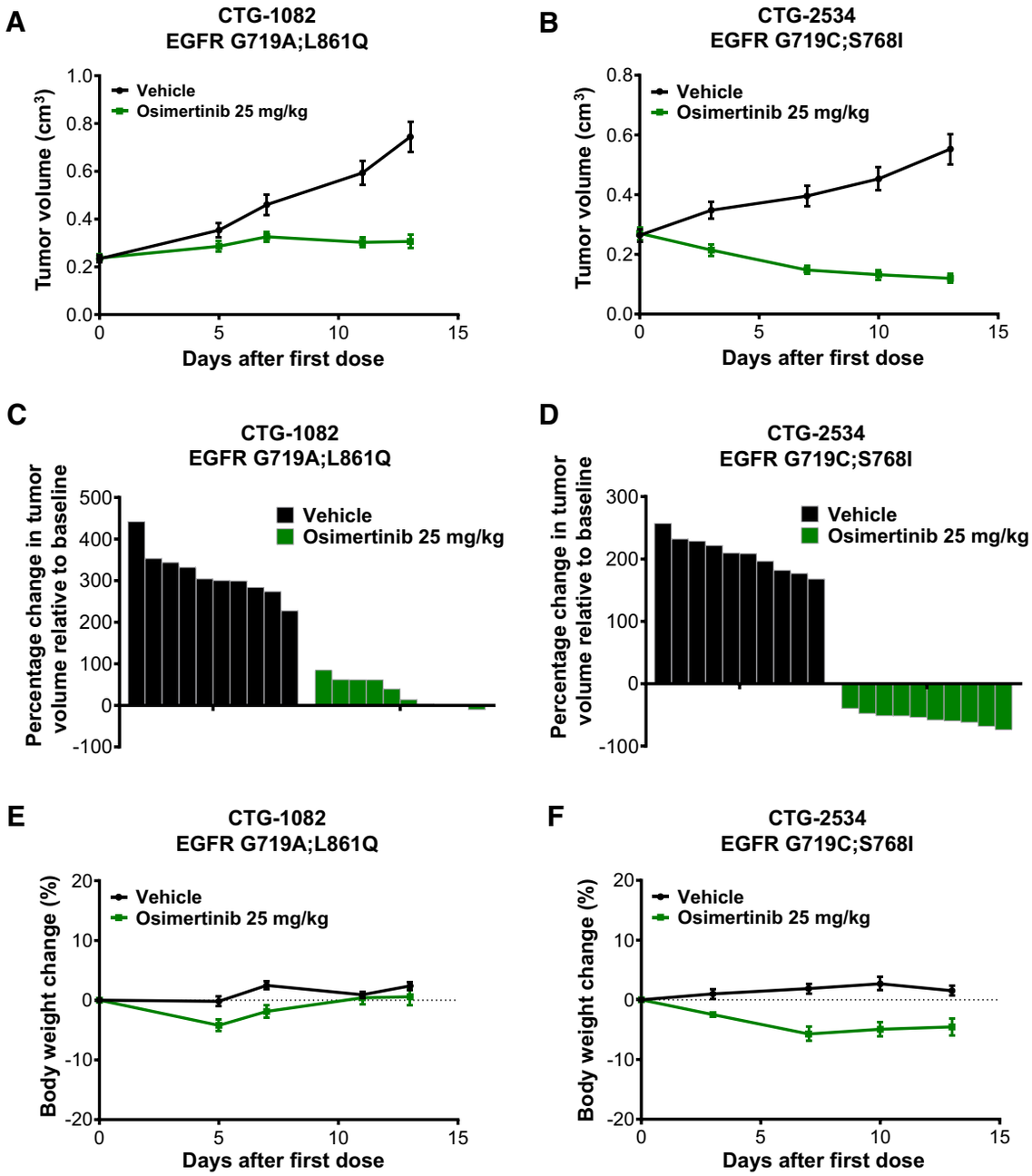

Figure 4.

Osimertinib monotherapy induces tumor growth inhibition in two NSCLC EGFR G719X complex mutation PDX models *in vivo*. **A** and **B,** Tumor growth inhibition following daily dosing of vehicle, osimertinib 25 mg/kg, or afatinib 7.5 mg/kg in the subcutaneous CTG-1082 or CTG-2534 PDX models in nude mice. **C** and **D,** Waterfall plot representing tumor volume of individual mice at the end of the treatment period. **E** and **F,** No significant body weight loss (less than 10% of starting body weight) is observed at these efficacious doses. Data expressed as a percentage change in nude mouse body weight relative to start size on day 0. Data are represented as mean ± SEM ($n = 10$ per group).

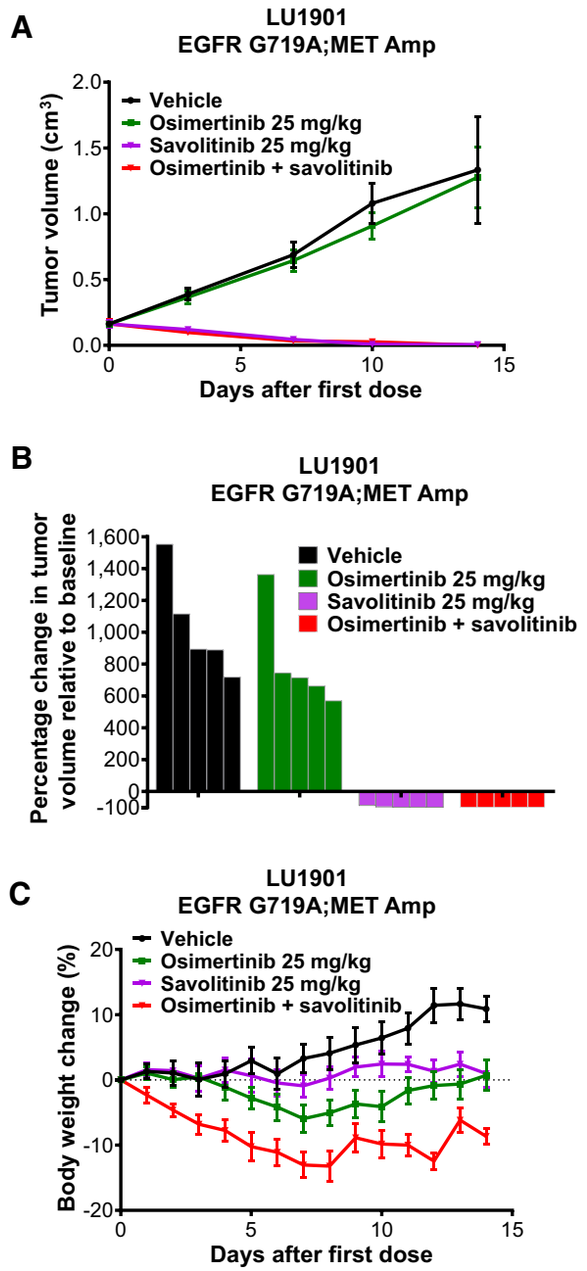

Figure 5:

Savolitinib overcomes resistance to osimertinib in an NSCLC EGFR G719A, which displays a MET amplification *in vivo*. **A,** Tumor growth inhibition following daily dosing of vehicle, osimertinib 25 mg/kg, savolitinib 25 mg/kg, or the combination of osimertinib and savolitinib in the subcutaneous LU1901 PDX models in nude mice. **B,** Waterfall plot representing tumor volume of individual mice at the end of the treatment period. **C**, No significant body weight loss (less than 10% of starting body weight) is observed at these efficacious doses. Data expressed as a percentage change in nude mouse body weight relative to start size on day 0. Data are represented as mean ± SEM ($n = 5$ per group).

administered savolitinib, a type 1 MET inhibitor (24), alone or in combination with osimertinib. Once-daily administration of 25 mg/kg of savolitinib alone or in combination with osimertinib induced profound tumor growth regression (>100; 95%, $P < 0.001$ at day 14; >100, 100%, $P < 0.001$ at day 14) when compared with the control group, respectively (**Fig. 5A**). Waterfall plots for each of the individual mice demonstrate that in the LU1901 PDX model, 3 of 5 mice and 5 of 5 mice had no measurable tumor growth when treated with savolitinib alone or with savolitinib in combination with osimertinib, respectively, at day 14 (**Fig. 5B**), whereas all the mice in the osimertinib-treated cohort had tumor growth similar to control-treated cohort by day 14 (**Fig. 5B**). Collectively, these results demonstrate that the growth of the LU1901 model EGFR-mutant, MET-amplified is dependent on MET activation alone.

Both compounds were well tolerated, and minimal body weight loss was observed compared with predose starting body weight (**Fig. 5C**).

Discussion

Despite the success of approved TKI therapies to treat NSCLC patients harboring activating mutations in EGFR, the benefit of treatment from these agents remains mostly limited to the common Ex19del and L858R mutant subtypes.

Alongside L858R and Ex19del, the uncommon EGFR mutations G719X, L861Q, and S768I account for 5% of EGFR mutations. This subgroup is less sensitive to first-generation TKI, erlotinib, and gefitinib. Patients with uncommon mutations had a significant shorter PFS and lower ORR than did patients with common mutations (PFS, 7.7 vs. 11.4 months; ORR, 41.6% vs. 66.5%; ref. 9). Retrospective review of the LUX-LUNG trials reveals that the ORR and PFS were very similar in between the uncommon patient population and the patient harboring canonical activating mutations following treatment with afatinib.

Previous reports have postulated the potential of osimertinib in the uncommon mutation setting; however, these studies were limited to using Ba/F3 engineered cell models *in vitro* (8, 15). We therefore wanted to take a more comprehensive approach to evaluating osimertinib across a wider range of uncommon mutations and using more disease-relevant models *in vitro* and *in vivo*. Using *in vitro* cell EGFR phosphorylation assays, we demonstrated the potency of osimertinib and AZ5104, its active metabolite, against a panel of single and compound, uncommon mutations; in all cases, the IC_{50} for inhibition of EGFR phosphorylation was less than 50 nmol/L for both compounds. We identified two patient-derived tumor cell lines and four PDX models that harbor an uncommon mutation, which allows us to evaluate osimertinib activity both *in vitro* and i*n vivo*. Using this approach, we were able to demonstrate *in vitro* that osimertinib inhibits EGFR phosphorylation and downstream signaling and translated into cell proliferation inhibition. The potency of these effects in PDX cell lines was consistent with the potency we observed in cell phosphorylation assays. *In vivo*, osimertinib delivered high levels of antitumor activity across PDX models at 25 mg/kg/day, a dose modeled to be approximately consistent with the 80-mg clinically approved dose for targeting the canonical Ex19 del and L858R mutations as well as the gatekeeper T790M tumors. Moreover, the level of efficacy achieved was significantly greater than clinically relevant doses of afatinib. The tumor inhibition activity of osimertinib was associated with potent activity against EGFR and downstream signaling pathways. Using this approach, we were able to demonstrate that osimertinib exerts profound tumor growth inhibition in tumor harboring uncommon mutations.

Of all the models evaluated, only the LU1901 model, EGFR-mutant and MET-amplified, was resistant to osimertinib. MET amplification is a well-established resistance mechanism known to bypass EGFR inhibition and impart resistance to EGFR-TKIs,

including osimertinib (23). This model was dependent on MET activation alone as no additional benefit of osimertinib addition to savolitinib was observed over savolitinib monotherapy. To note, some recent reports have also described monotherapy MET inhibitor sensitivity in EGFR-mutant patients, suggesting that single-agent MET dependence can also occur clinically in patients (25, 26).

In parallel, to evaluate all the uncommon G719X, L861Q, and S768I mutations, single or compound mutation forms not represented in the two-patient-derived tumor cell lines and the four PDX models, we used an *in vitro* cellular EGFR phosphorylation assay. In the assay, osimertinib demonstrated potent inhibition against all the uncommon mutations evaluated at potencies comparable to the common activating ex19del and L858R mutants.

Recently, a paper by Ahn and colleagues shows that osimertinib demonstrated favorable activity with manageable toxicity in patients with NSCLC harboring uncommon EGFR mutations (10). Thirty-six patients with uncommon mutations were evaluated, and the objective response rate was 50% with a median PFS of 8.2 months. Although cross-trial comparisons should be performed with caution, the activity of osimertinib seems to be superior against the activating mutations. The objective response rate was 80% with a median PFS of 17.2 months (20). However, larger studies in patients harboring uncommon mutations will be required to evaluate this further.

Overall, we suggest the work presented here, in addition to the first clinical report, provides sufficient evidence to warrant additional clinical testing of osimertinib within this uncommon EGFR mutation population to establish whether osimertinib can offer improved clinical benefit in this important remaining area of unmet need as a differentiated next-generation TKI.

Disclosure of Potential Conflicts of Interest

D.A.E. Cross reports personal fees from AstraZeneca (employer) outside the submitted work. B.C. Cho reports grants from Novartis, Bayer, AstraZeneca, MOGAM Institute, Dong-A ST, Champions Oncology, Janssen, Yuhan, Ono, Dizal Pharma, MSD, AbbVie, Medpacto, GIInnovation, Eli Lilly, and Blueprint Medicines (research funding), personal fees from Novartis, AstraZeneca, Boehringer-Ingelheim, Roche, BMS, Ono, Yuhan, Pfizer, Eli Lilly, Janssen, Takeda, MSD, Janssen, Medpacto, and Blueprint Medicines (consulting), personal fees from TheraCanVac Inc, Gencurix Inc, Bridgebio Therapeutics, KANAPH Therapeutic Inc (stock ownership), personal fees from KANAPH Therapeutic Inc (scientific advisory board), other from Daan Biotherapeutics (founder), and other from Champions Oncology (royalty) outside the submitted work. P.D. Smith reports other from AstraZeneca PLC (employee and shareholder) outside the submitted work. No potential conflicts of interest of were disclosed by the other authors.

Authors' Contributions

N. Floc'h: Conceptualization, data curation, formal analysis, supervision, investigation, methodology, and writing–original draft. **S. Lim:** Conceptualization, data curation, formal analysis, supervision, and methodology. **S. Bickerton:** Resources, formal analysis, and methodology. **A. Ahmed:** Resources, formal analysis, and methodology. **J. Orme:** Resources, formal analysis, and methodology. **J. Urosevic:** Resources, formal analysis, and methodology. **M.J. Martin:** Supervision, writing–review, and editing. **D.A.E. Cross:** Supervision. **B.C. Cho:** Writing–review and editing. **P.D. Smith:** Writing-review and editing.

The costs of publication of this article were defrayed in part by the payment of page charges. This article must therefore be hereby marked *advertisement* in accordance with 18 U.S.C. Section 1734 solely to indicate this fact.

Received February 12, 2020; revised May 22, 2020; accepted August 26, 2020; published first September 17, 2020.

References

1. Roengvoraphoj M, Tsongalis GJ, Dragnev KH, Rigas JR. Epidermal growth factor receptor tyrosine kinase inhibitors as initial therapy for non-small cell lung cancer: focus on epidermal growth factor receptor mutation testing and mutation-positive patients. Cancer Treat Rev 2013;39:839–50.
2. Sharma SV, Bell DW, Settleman J, Haber DA. Epidermal growth factor receptor mutations in lung cancer. Nat Rev Cancer 2007;7:169–81.
3. Beau-Faller M, Prim N, Ruppert AM, Nanni-Metellus I, Lacave R, Lacroix L, et al. Rare EGFR exon 18 and exon 20 mutations in non-small-cell lung cancer on 10 117 patients: a multicentre observational study by the French ERMETIC-IFCT network. Ann Oncol 2014;25:126–31.
4. Costa DB. Kinase inhibitor-responsive genotypes in EGFR mutated lung adenocarcinomas: moving past common point mutations or indels into uncommon kinase domain duplications and rearrangements. Transl Lung Cancer Res 2016; 5:331–7.
5. Kobayashi Y, Mitsudomi T. Not all epidermal growth factor receptor mutations in lung cancer are created equal: Perspectives for individualized treatment strategy. Cancer Sci 2016;107:1179–86.
6. O'Kane GM, Bradbury PA, Feld R, Leighl NB, Liu G, Pisters KM, et al. Uncommon EGFR mutations in advanced non-small cell lung cancer. Lung Cancer 2017;109:137–44.
7. Tu HY, Ke EE, Yang JJ, Sun YL, Yan HH, Zheng MY, et al. A comprehensive review of uncommon EGFR mutations in patients with non-small cell lung cancer. Lung Cancer 2017;114:96–102.
8. Kohsaka S, Nagano M, Ueno T, Suehara Y, Hayashi T, Shimada N, et al. A method of high-throughput functional evaluation of EGFR gene variants of unknown significance in cancer. Sci Transl Med 2017;9:eaan6566.
9. Chiu CH, Yang CT, Shih JY, Huang MS, Su WC, Lai RS, et al. Epidermal growth factor receptor tyrosine kinase inhibitor treatment response in advanced lung adenocarcinomas with G719X/L861Q/S768I mutations. J Thorac Oncol 2015; 10:793–9.
10. Cho JH, Lim SH, An HJ, Kim KH, Park KU, Kang EJ, et al. Osimertinib for patients with non-small-cell lung cancer harboring uncommon egfr mutations: a multicenter, open-label, phase II Trial (KCSG-LU15-09). J Clin Oncol 2020;38: 488–95.
11. Fukihara J, Watanabe N, Taniguchi H, Kondoh Y, Kimura T, Kataoka K, et al. Clinical predictors of response to EGFR tyrosine kinase inhibitors in patients with EGFR-mutant non-small cell lung cancer. Oncology 2014;86: 86–93.
12. Watanabe S, Minegishi Y, Yoshizawa H, Maemondo M, Inoue A, Sugawara S, et al. Effectiveness of gefitinib against non-small-cell lung cancer with the uncommon EGFR mutations G719X and L861Q. J Thorac Oncol 2014;9: 189–94.
13. Wu JY, Yu CJ, Chang YC, Yang CH, Shih JY, Yang PC. Effectiveness of tyrosine kinase inhibitors on "uncommon" epidermal growth factor receptor mutations of unknown clinical significance in non-small cell lung cancer. Clin Cancer Res 2011;17:3812–21.
14. Yang JC, Sequist LV, Geater SL, Tsai CM, Mok TS, Schuler M, et al. Clinical activity of afatinib in patients with advanced non-small-cell lung cancer harbouring uncommon EGFR mutations: a combined post-hoc analysis of LUX-lung 2, LUX-lung 3, and LUX-lung 6. Lancet Oncol 2015;16:830–8.
15. Cross DA, Ashton SE, Ghiorghiu S, Eberlein C, Nebhan CA, Spitzler PJ, et al. AZD9291, an irreversible EGFR TKI, overcomes T790M-mediated resistance to EGFR inhibitors in lung cancer. Cancer Discov 2014;4:1046–61.
16. Mok TS, Wu YL, Ahn MJ, Garassino MC, Kim HR, Ramalingam SS, et al. Osimertinib or platinum-pemetrexed in EGFR T790M-positive lung cancer. N Engl J Med 2017;376:629–40.
17. Reungwetwattana T, Nakagawa K, Cho BC, Cobo M, Cho EK, Bertolini A, et al. CNS response to osimertinib versus standard epidermal growth factor receptor tyrosine kinase inhibitors in patients with untreated egfr-mutated advanced non-small-cell lung cancer. J Clin Oncol 2018:JCO2018783118.
18. Soria JC, Ohe Y, Vansteenkiste J, Reungwetwattana T, Chewaskulyong B, Lee KH, et al. Osimertinib in untreated EGFR-mutated advanced non-small-cell lung cancer. N Engl J Med 2018;378:113–25.

19. Wu YL, Ahn MJ, Garassino MC, Han JY, Katakami N, Kim HR, et al. CNS efficacy of osimertinib in patients with T790M-positive advanced non-small-cell lung cancer: data from a randomized phase III trial (AURA3). J Clin Oncol 2018; 36:2702–9.
20. Ramalingam SS, Vansteenkiste J, Planchard D, Cho BC, Gray JE, Ohe Y, et al. Overall survival with osimertinib in untreated, EGFR-mutated advanced NSCLC. N Engl J Med 2020;382:41–50.
21. Yun J, Hong MH, Kim SY, Park CW, Kim S, Yun MR, et al. YH25448, an irreversible EGFR-TKI with potent intracranial activity in EGFR mutant non-small cell lung cancer. Clin Cancer Res 2019;25: 2575–87.
22. Finlay MR, Anderton M, Ashton S, Ballard P, Bethel PA, Box MR, et al. Discovery of a potent and selective EGFR inhibitor (AZD9291) of both sensitizing and T790M resistance mutations that spares the wild type form of the receptor. J Med Chem 2014;57:8249–67.
23. Yang M, Shan B, Li Q, Song X, Cai J, Deng J, et al. Overcoming erlotinib resistance with tailored treatment regimen in patient-derived xenografts from naive Asian NSCLC patients. Int J Cancer 2013;132:E74–84.
24. Schuller AG, Barry ER, Jones RD, Henry RE, Frigault MM, Beran G, et al. The MET inhibitor AZD6094 (savolitinib, HMPL-504) induces regression in papillary renal cell carcinoma patient-derived xenograft models. Clin Cancer Res 2015;21:2811–9.
25. Ou SI, Agarwal N, Ali SM. High MET amplification level as a resistance mechanism to osimertinib (AZD9291) in a patient that symptomatically responded to crizotinib treatment post-osimertinib progression. Lung Cancer 2016;98:59–61.
26. Yoshimura K, Inui N, Karayama M, Inoue Y, Enomoto N, Fujisawa T, et al. Successful crizotinib monotherapy in EGFR-mutant lung adenocarcinoma with acquired MET amplification after erlotinib therapy. Respir Med Case Rep 2017; 20:160–3.